Supporting Information

Performance Leap of Lithium Metal Batteries in $LiPF_6$ Carbonate Electrolyte by a Phosphorus Pentoxide Acid Scavenger

Jian Zhang,[1,#] Jiayan Shi,[2,3,#] Leo W. Gordon,[4] Nastaran Shojarazavi,[2] Xiaoyu Wen,[2] Yifan Zhao,[1] Jianjun Chen,[2] Chi-Cheung Su,[3] Robert J. Messinger,[4,] Juchen Guo[1,2,*]*

[1]Materials Science and Engineering Program, University of California – Riverside, Riverside, CA 92521, USA
[2]Department of Chemical and Environmental Engineering, University of California – Riverside, Riverside, CA 92521, USA
[3]Chemical Sciences and Engineering Division, Argonne National Laboratory, Lemont, IL 60439, USA
[4]Department of Chemical Engineering, The City College of New York, CUNY, New York, NY 10031, United States

AUTHOR INFORMATION

Corresponding Author

[*]E-mail: rmessinger@ccny.cuny.edu; jguo@engr.ucr.edu

[#]These authors contribute equally.

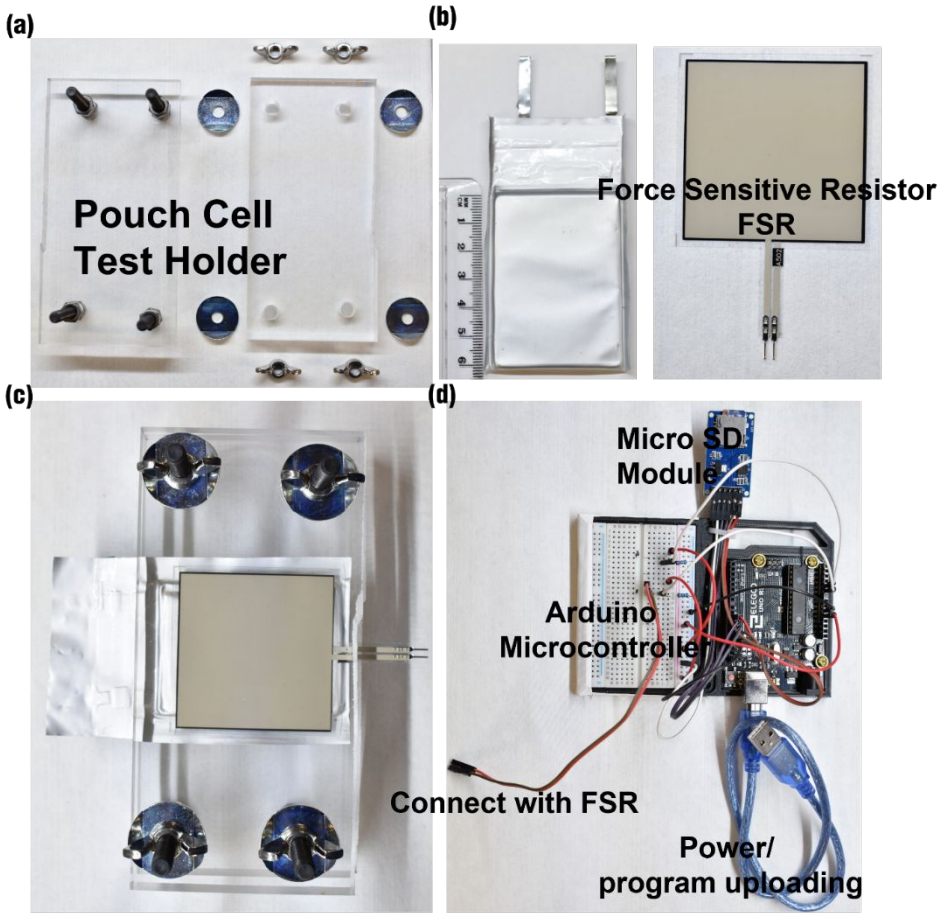

Figure S1. Photographs of (a) pouch cell testing holder, (b) force sensitive resistor, (c) assembled testing holder, and (d) pressure loading calibration by a (d) Arduino microcontroller.

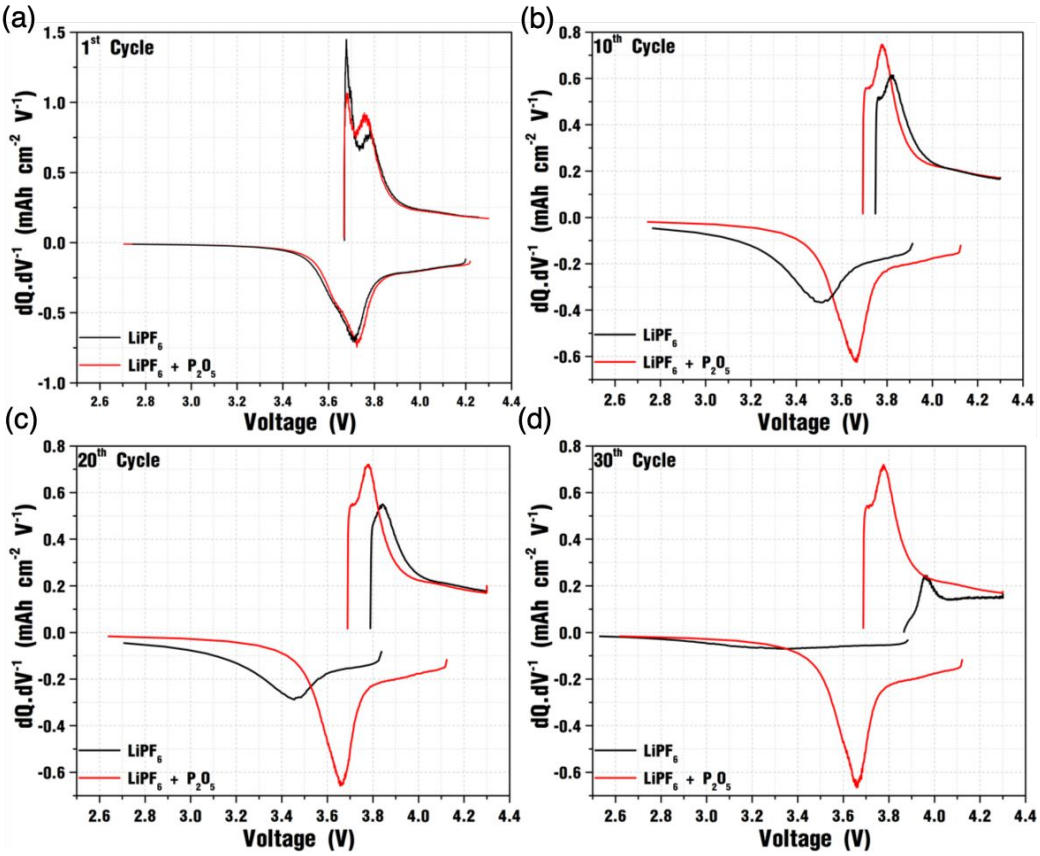

Figure S2. Differential capacity (dQ/dV vs. voltage) plots comparing the commercial (black) and P_2O_5-modified (red) $LiPF_6$ electrolytes during the (a) 1st cycle, (b) 10th cycle, (c) 20th cycle, and (d) 30th cycle. The major redox peaks for the cell using the commercial electrolyte shift to higher voltages during charge (from 3.76 V in the 1st cycle to 3.96 V in the 30th cycle) and lower voltages during discharge (from 3.71 V in the 1st cycle to 3.27 V in the 30th cycle). However, the redox peaks for the cell using the P_2O_5 -modified electrolyte do not shift upon galvanostatic cycling.

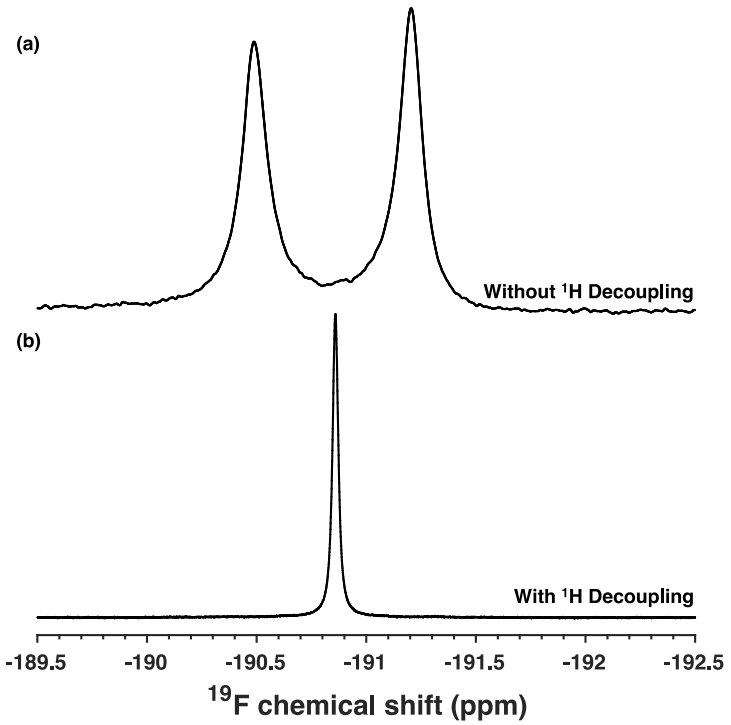

Figure S3. Liquid-state ^{19}F single-pulse NMR measurements in the HF region (a) without and (b) with ^{1}H-^{19}F heteronuclear decoupling, both performed on the commercial 1 M $LiPF_6$ electrolyte.

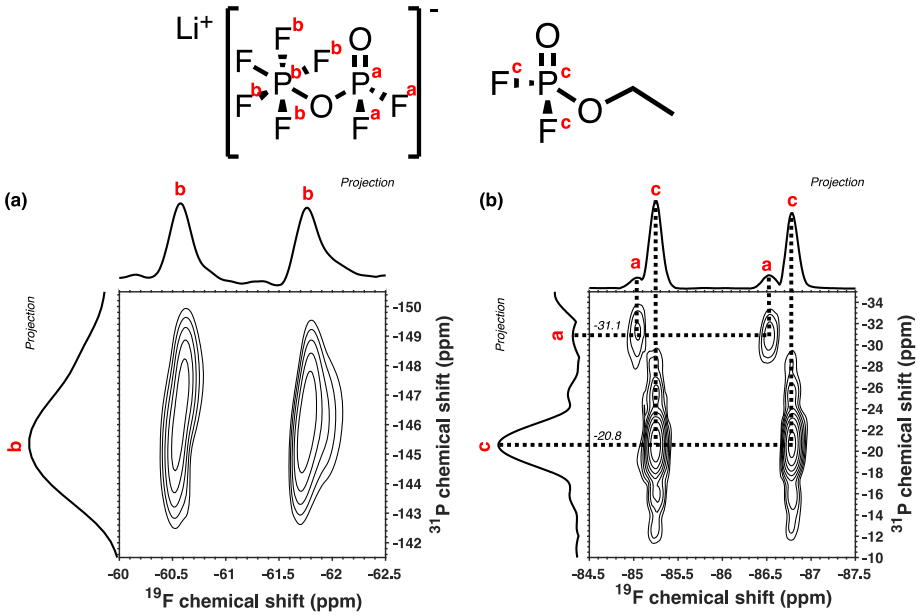

Figure S4. Liquid-state 2D $^{19}F\{^{31}P\}$ HMQC through-bond correlation NMR measurements on the P_2O_5-modifed $LiPF_6$ electrolyte, which establishes interactions between (a) the ^{19}F doublet at -61.1 ppm and ^{31}P signal at approximately -146 ppm, as well as (b) the ^{19}F doublet centered at -85.7 ppm and ^{31}P signal at -31.1 ppm. These ^{19}F-^{31}P through-bond correlation experiments confirm the existence of the $OPF_2OPF_5^-$ anions (species "D" in **Figure 2** and **Table 1,** main article). Additionally, the region in (b) shows the ^{19}F-^{31}P through-bond correlation between the ^{19}F signal centered at -86.0 ppm and ^{31}P signal at -20.8 ppm, associated with $C_2H_5OPOF_2$ (species "E" in **Figure 2** and **Table 1**, main article). Chemical structures of these electrolyte species are labeled with ^{19}F and ^{31}P signal assignments.

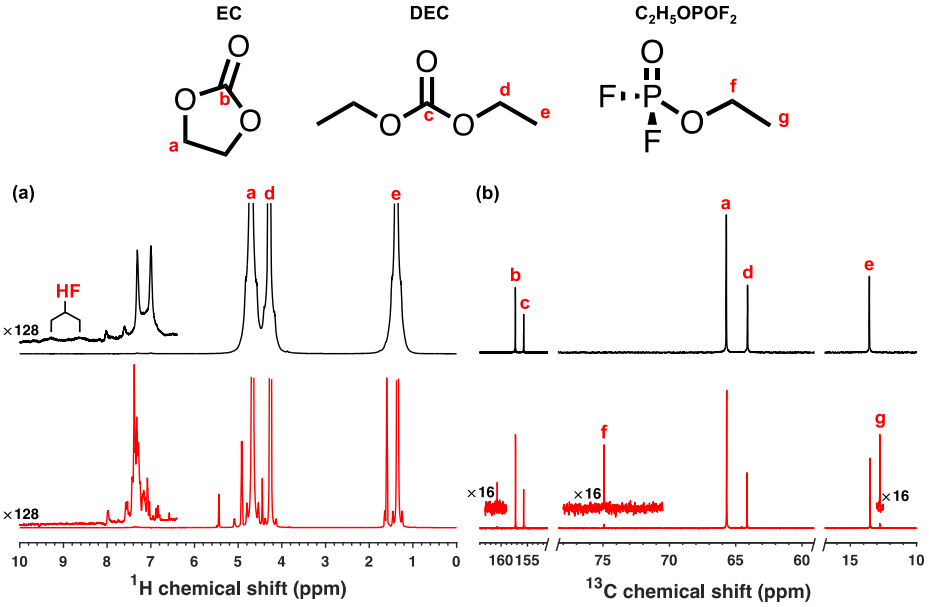

Figure S5. Liquid-state (a) ^{1}H, and (b) ^{13}C single-pulse NMR measurements of the commercial (black) and P_2O_5-modifed (red) 1 M $LiPF_6$ electrolyte in EC/DEC (50/50 v/v). Integration of the relative ^{13}C signal intensities reveal that the molar ratio of DEC:EC is 0.57:1.0 and 0.37:1.0 in the commercial and P_2O_5-modified electrolyte, respectively, establishing that DEC is the major source for organic species in the reaction products generated from P_2O_5. Chemical structures of major proton- and carbon-containing electrolyte species are labeled with ^{1}H and ^{13}C signal assignments.

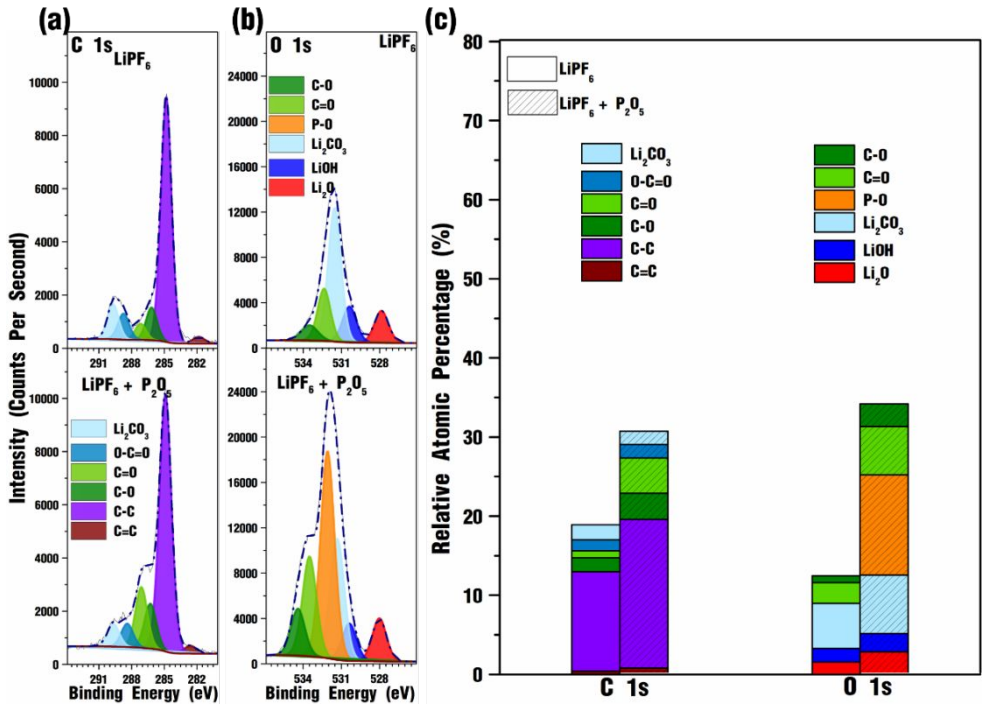

Figure S6. (a) C 1s and (b) O 1s XPS spectra of the Li metal surface after immersion in the commercial (top) or P_2O_5-modified (bottom) $LiPF_6$ electrolyte for 48 hours. (c) Relative atomic percentage of C and O atoms on the surfaces.

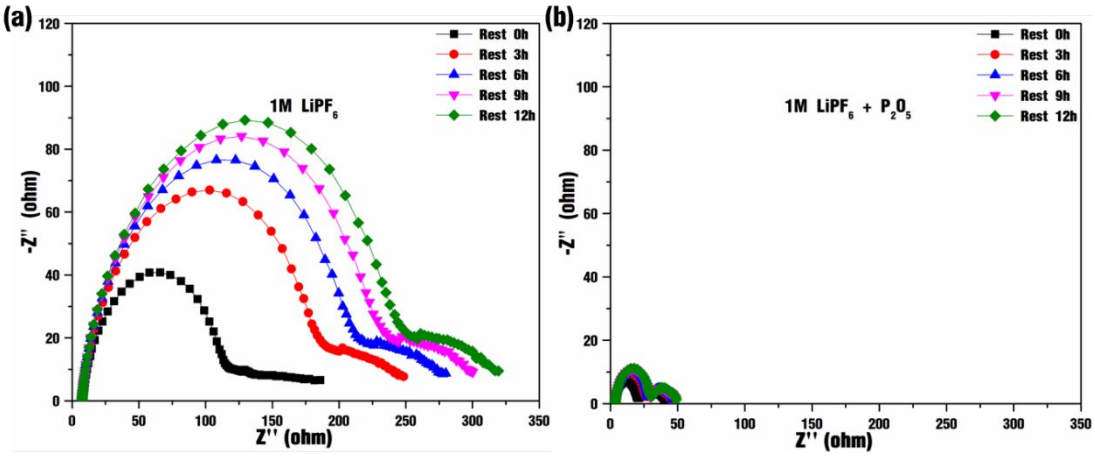

Figure S7. EIS Nyquist plots performed at different rest times in Li||Li symmetric cells in (a) commercial or (b) P_2O_5-modified $LiPF_6$ electrolyte. The EIS data was analyzed by ZSim software to deconvolute the circuit elements using the equivalent circuit model displayed below.

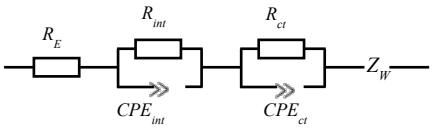

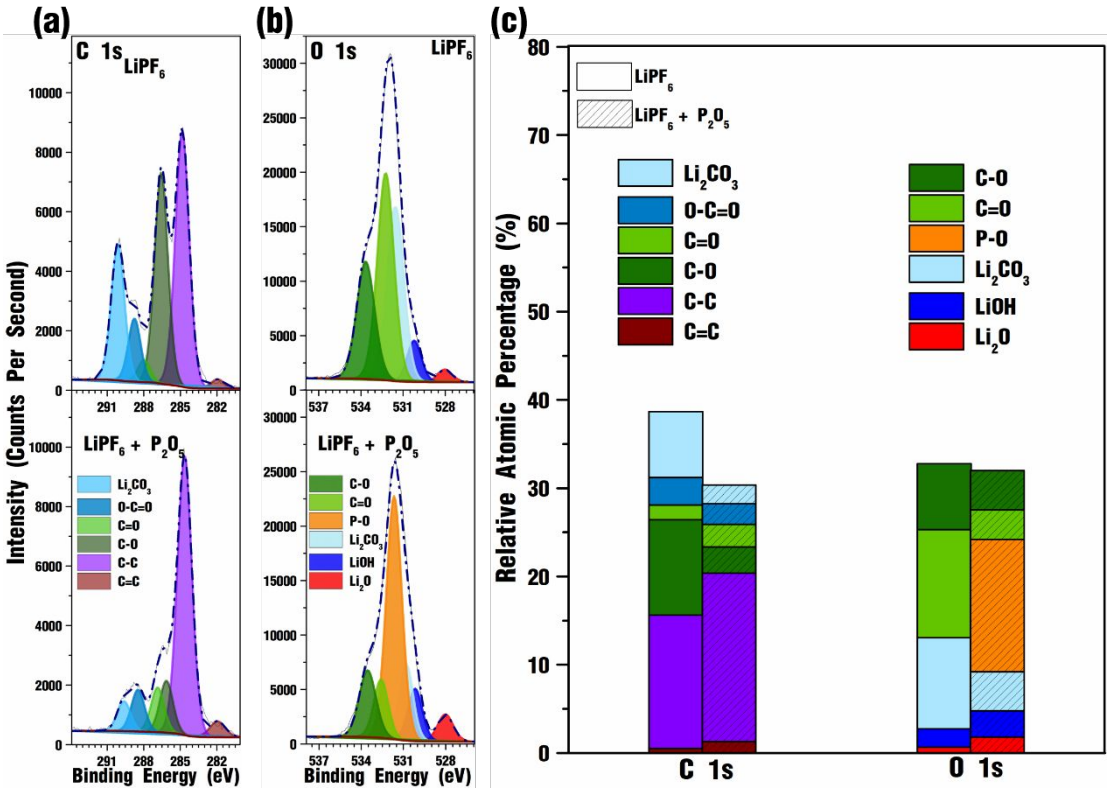

Figure S8. (a) C 1s, (b) O 1s, (c) Li 1s XPS spectra, of the Li metal surface after galvanostatic deposition (0.3 mA cm^{-2}) for 10 hours in commercial or P_2O_5-modified 1 M $LiPF_6$ electrolyte. (c) Relative atomic percentage of C and O atoms on the surfaces.

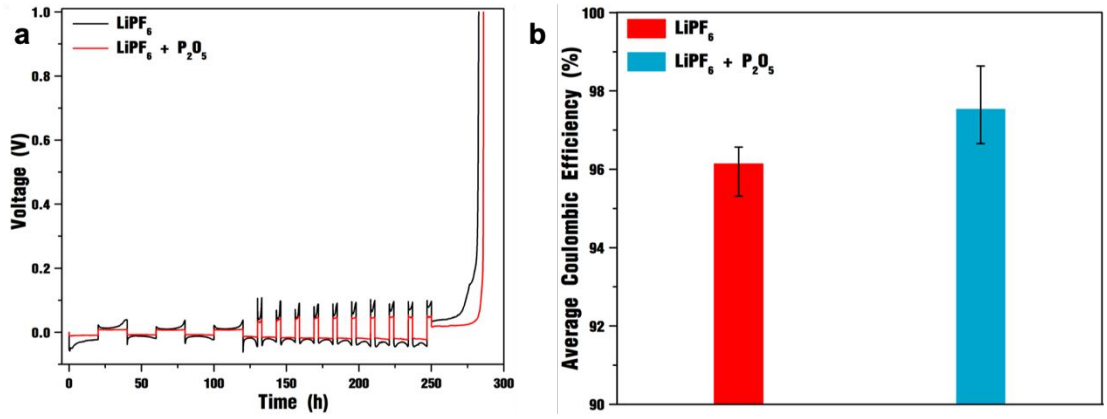

Figure S9. (a) The representative Li deposition and stripping curves to measure the CE and (b) The average CE of Li deposition-stripping measured from the pristine and P_2O_5-modified $LiPF_6$ electrolyte.

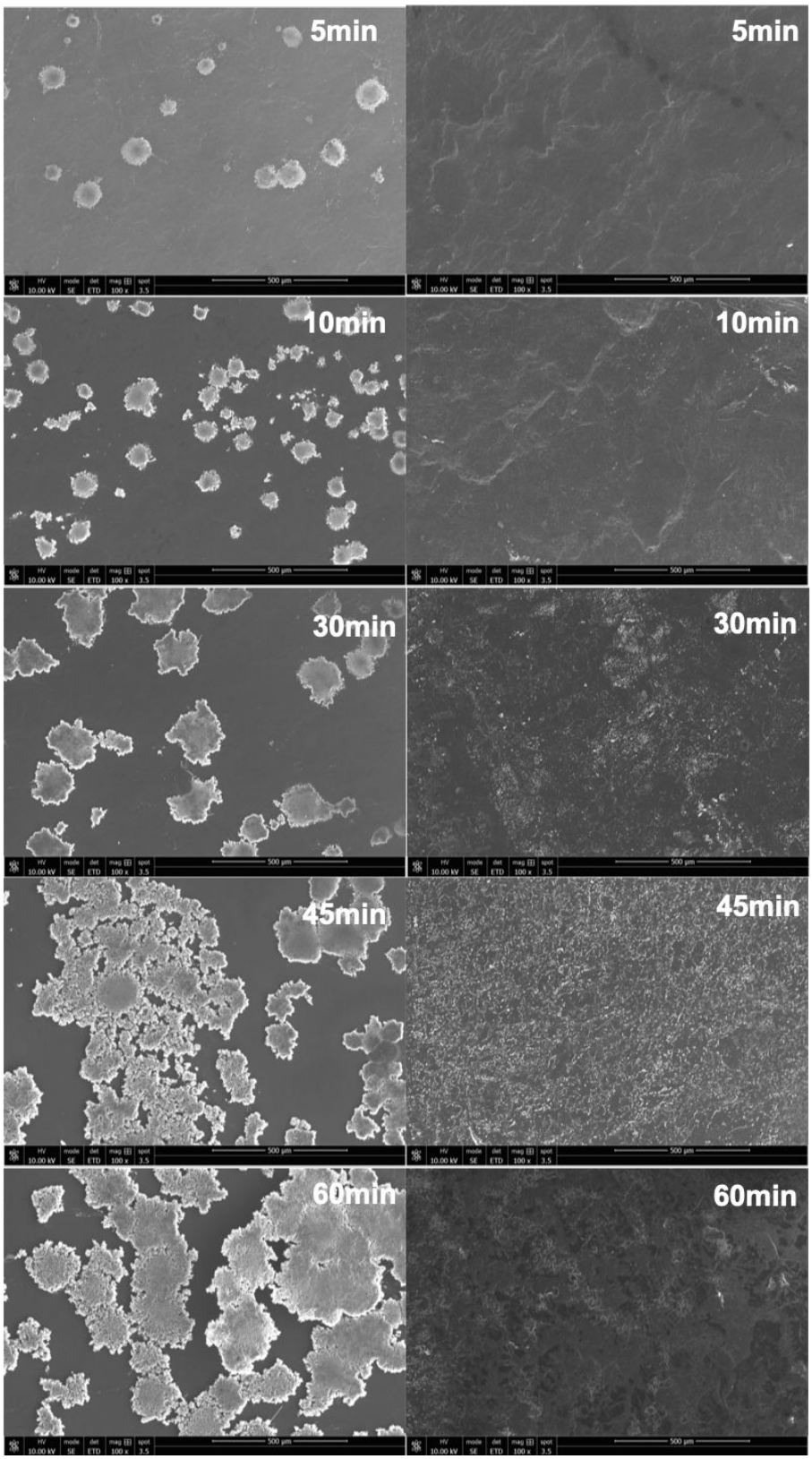

Figure S10. Left column: Li depostion from the pristine $LiPF_6$ electrolyte; Right column: Li depsotion from the P_2O_5-modified $LiPF_6$ electrolyte.

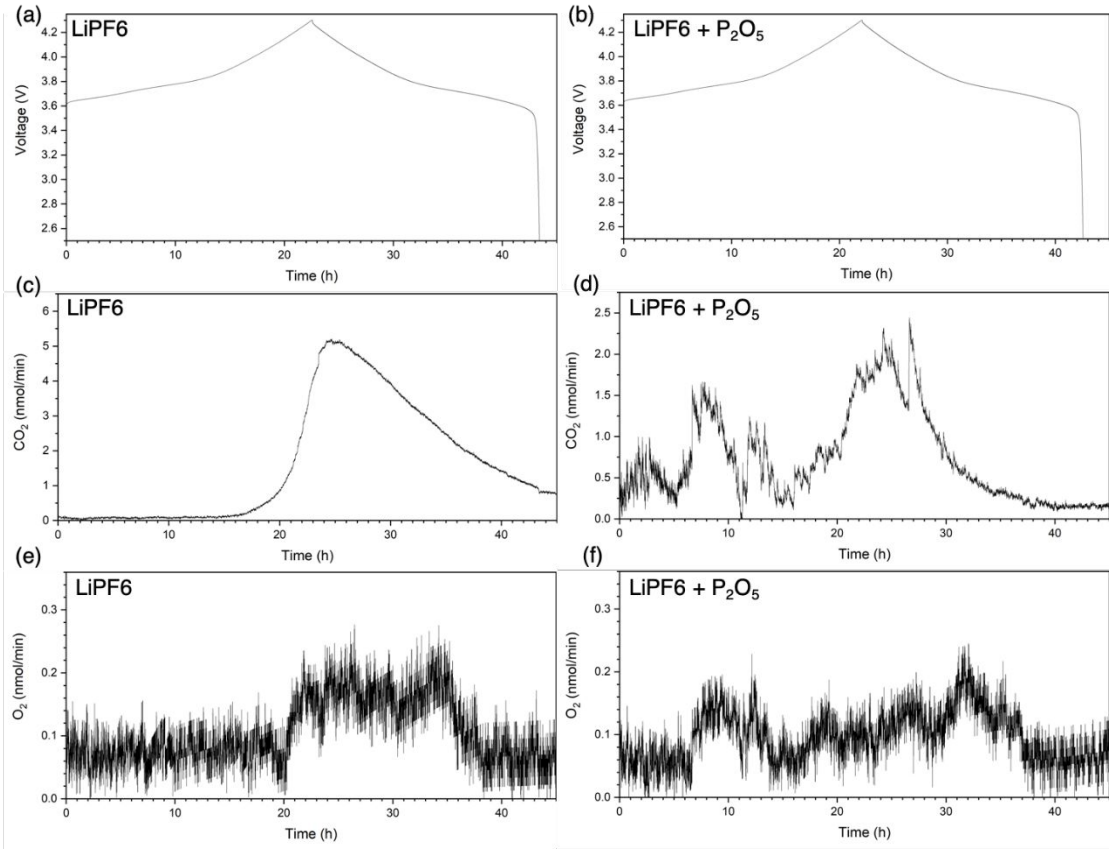

Figure S11. Gas analysis using DEMS. (a, b) Charge-discharge curves, (c, d) CO_2 generation rate and (e, f) O_2 generation rate with commercial $LiPF_6$ electrolyte and the electrolyte modified by P_2O_5.